The application of electrical resistance measurements to water transport in lime-masonry systems

R J Ball[1,2*], G C Allen[2], M A Carter[3], M A Wilson[3], C Ince[3], A El-Turki[2]

[1] Currently: Department of Architecture and Civil Engineering, University of Bath, Bath, BA2 7AY, UK

[2] Interface Analysis Centre, University of Bristol, Bristol, BS2 8BS, UK

[3] School of Mechanical, Aerospace and Civil Engineering, University of Manchester, PO Box 88, Manchester M60 1QD, UK

**Corresponding author*

Abstract

The paper describes an experimental determination of impedance spectroscopy derived resistance measurements to record water transport in lime-masonry systems. It strongly supports the use of Sharp Front theory and Boltzmann's distribution law of statistical thermodynamics to corroborate the data obtained. A novel approach is presented for the application of impedance measurements to the water transport between freshly mixed mortars and clay brick substrates. Once placed, fresh mortar is dewatered by brick and during this time the volume fraction water content of the mortar is reduced. An equation is derived relating this change in water content to the bulk resistance of the mortar. Experimental measurements on hydraulic lime mortars placed in contact with brick prisms confirm the theoretical predictions. Further, the results indicate the time at which dewatering of a mortar bed of given depth is completed. The technique has then potential to be applied for in situ monitoring of dewatering as a means of giving insight into the associated changes in mechanical and chemical properties.

Key words: Impedance spectroscopy, Boltzmann's distribution law, water transport

1. Introduction

When a freshly mixed mortar in the form of render or jointing mortar is applied to an absorbent substrate such as clay brick, water is abstracted from the wet mix by the capillary suction of the substrate. This process has important implications for the subsequent strength development and engineering properties of the material [1,2]. The extent to which water is removed from the wet mix depends on both the sorptivity of the substrate and the water retaining ability (desorptivity) of the mortar [3,4]. This initial dewatering prior to setting is likely to have a significant influence on the long term durability of the mortar in terms of its mechanical strength and its resistance to environmental degradation and frost damage. The ability to monitor dewatering non-destructively is therefore of great importance in providing an insight to the long term performance of these materials.

The application of NHL mortars in the conservation, restoration, renovation and new build sectors of construction is growing rapidly. As their name implies NHLs set by reacting with water in a similar manner to cements. Compared with Portland cement NHL's have lower strength but provide for greater movement [5]. This and a number of other desirable properties make them better suited in many applications [6-8]. In the present study natural hydraulic lime (NHL) mortars in the freshly mixed state were investigated after placing on initially dry clay common facing brick.

This paper reports the use of impedance spectroscopy to monitor the dewatering of mortars prior to the early stages of the setting process. Phase angle measurements were taken over a range of frequencies and complex plane plots of imaginary versus real impedance were interpreted in terms of equivalent circuit parameters.

The application of impedance spectroscopy to cementitious materials has been developed by McCarter, among others [9-13]. Previous work in this area has concentrated on the use of impedance spectroscopy to study hydraulic or pozzolanic reactions during setting.

Recent work by Ball *et. al.* investigating physio-chemical processes in lime-based composites demonstrated that impedance spectroscopy can track a carbonation front in natural hydraulic lime mortar using an electrode array [14].

These studies have allowed a number of fundamental properties to be linked to the impedance response of a cementitious material in the set and hardened state. Such properties include pore water content, pore water ionic concentration, and porosity and tortuosity of the pore network. The following can be deduced from the literature on resistivity measurments in hardened cement mortars [13]:

- Resistivity decreases with the amount of evaporable water in the cement paste.
- Resistivity decreases with the concentration of mobile ions in the pore fluid.
- Resistivity is influenced by the connectivity (or tortuosity) of the pore network.

The impedance behaviour of hydraulic lime mortars in the freshly mixed state however has not as yet been investigated although alkali activated slag binders (from 15 minutes after mixing) and cement has not as yet been studied [11]. Results from these studies attribute changes in conductance during the first hour after mixing to an increase in ionic concentration following dissolution of soluble species from the binder into the mix water. Portland cement based binders showed changes in conductivity during the first hour followed by a dormant period lasting approximately 9 hours. A large change following this dormant period signified intense chemical activity due to hydration reactions [13]

There are few reports in the literature addressing the application of impedance measurements to monitor changes occurring in freshly mixed wet mortars following placement in contact with absorbent substrates. This may be a reflection of the experimental difficulties involved in the measurement of relatively thin layers of mortar, or that this early dewatering has been completely overlooked. It has been found [15] that between 40 and 60 % by volume of the mix water is abstracted from freshly mixed lime under the capillary pressure of dry clay brick. On site, bricks and other masonry units

will not be oven dry and so will abstract less. Nevertheless this dewatering has a significant effect on mortar strength [1] and probably on durability.

The relationship between saturation and electrical conductivity in porous media has been investigated by Hunt, for unsaturated systems, using an Archie's law approach [16]. He applied a continuum percolation theory to previously published data representing the full range of saturation. This included data obtained from sandstone, fine sandy loam, soil (consisting various ratios of sand and clay), and various types of sand. The analysis demonstrated the ability to provide good predictions and was robust in respect to secondary effects such as residual salinity and contact resistance. The correlation between electrical resistivity and soil-water content using artificial intelligence techniques has been investigated by Ozcep and co-workers [17, 18]

Water content estimation by electrical measurement of soils offers new opportunities in geotechnical and agricultural studies. Techniques including time domain reflectometry [19, 20], high-frequency capacitance sensing [21] and resistivity cone penetration testing [22] have been applied. A useful theoretical approach to the dewatering of mortars, and slurries in general, is offered by a Sharp Front model which has its origins in soil science [3]. In this model it is assumed that a wetting front of uniform water content moves into the absorbent substrate from the wet mix and that there is a sharp boundary between the wetted and the dry regions. As dewatering proceeds, a filter cake of higher volume fraction solids content than the original mortar mix forms at the interface with the substrate. This interface progresses through the slurry until all the mortar has been converted to filter cake. This model is shown diagrammatically in Figure 2(b), discussed later.

2. Theory

The Sharp Front model developed by Hall and Hoff [3] describes the relationship between the sorptivity, S, of the substrate, the desorptivity, R, of the wet mix (in this case

freshly-mixed mortar) and the transfer sorptivity, A, between the wet mix and substrate by

$$\frac{1}{A^2} = \frac{1}{R^2} + \frac{1}{S^2} \qquad 1$$

This relationship has recently been experimentally validated [23]. The withdrawal of water from a wet mix by an initially dry substrate occurs by capillary action. As the wet mix is dewatered a filter cake forms at the boundary between the wet mix and substrate. As dewatering proceeds the filter cake increases in depth until all the wet mix has been converted to cake. The application of Darcy's law to the filter cake yields

$$\frac{di}{dt} = -K_c \frac{\Psi_i}{L_c} = -K_c \frac{\alpha \Psi_i}{\beta_i} \qquad 2$$

where i is the cumulative volume of water desorbed per unit area of wet mix in contact with the substrate, t the elapsed time, K_c the saturated permeability of the filter cake, Ψ_i the capillary potential of the substrate, L_c the depth of the filter cake and α and β are constants defined by the volume fraction water and solids contents of the wet mix and filter cake respectively [16]. Integration of equation 2 with respect to time gives

$$i = \left(\frac{2K_c |\Psi_i| \alpha}{\beta} \right)^{\frac{1}{2}} t^{\frac{1}{2}} = R t^{\frac{1}{2}} \qquad 3$$

where R is the desorptivity of the wet mix.

If the initial volume fraction of mix water is θ_0, then the volume fraction, θ, at any time t is given by

$$\theta = \theta_0 - i\, A_{sub}\,. \qquad 4$$

where A_{sub} is the area of wet mix in contact with substrate.

When a solid of charged surface is in contact with a liquid containing ions a double layer is formed at the surface. This layer is comprised of a tightly bound layer of fairly immobile ions adjacent to the solid and an oppositely charged ionic atmosphere [24]. The potential energy of ion species dissolved in the mix water may be related to the number of ions by Boltzmann's distribution law of statistical thermodynamics [25] giving

$$\frac{N_i}{N_j} = \exp^{\left[-\left(E_i - E_j\right)/kT\right]} \qquad 5$$

where N_i and N_j are the numbers of constituent ions in states i and j and E_i and E_j are the respective potential energies; k is Boltzmann's constant and T the absolute temperature. We suggest that when the mix water comes into contact with un-dissolved lime or sand particles a double layer is formed at the solid surface. In practice this layer will be very complex consisting of different ions, both positively and negatively charged. Tschapek reports that in the presence of water quartz sands undergo hydroxylation and charging instantaneously [26]. In the presence of water Si-O-Si bonds at the sand surface will react to form $2Si\text{-}O^{-}H^{+}$ resulting in a negatively charged surface. Chemical compounds originating from the lime will introduce ions such as Ca^{2+}, OH^{-} in addition to a range of metal ions. For the purpose of this analysis we assume a simple system where state i corresponds to ions within the double layer, and state j to ions in the mix water bulk. The development of a more complex analysis is beyond the scope of the current study. Nielsen applies a similar approach to soil and expresses the difference in energy between the two states by

$$E_i - E_j = ze\left(\varphi_i - \varphi_j\right) \qquad 6$$

where φ_i and φ_j are the electrical potentials of states i and j, e the charge on the electron and z the summary valence of the ions [27]. Combining equations 5 and 6 gives

$$\frac{N_i}{N_j} = \exp\left[- ze\left(\varphi_i - \varphi_j\right) \Big/ kT \right]. \qquad 7$$

If the volume fraction water content of the wet mix is changed by dewatering and the total surface area of solids is assumed to stay the same, then the total number of ions in the water bulk will decrease while those in the double layer will remain constant. Therefore the ratio N_i/N_j will be proportional to the volume fraction water content of the mortar, θ. The electrical potential difference, $(\varphi_i - \varphi_j)$, can be related to resistance, R_b by ohm's law therefore allowing the general expression

$$\theta = a \exp\left(- bR_b\right) \qquad 8$$

to be derived where a and b are empirical constants. Constant b is a function of z, T, electrical current and sample geometry. Values of a and b are discussed in the results and discussion section. Equation 8 shows that the volume fraction water content is directly proportional to the function $\exp(-bR_b)$ and that bulk resistance should increase as the water content of the mix decreases. Substitution of equations 3 and 8 into equation 4 gives

$$a \exp\left(- bR_b\right) = \theta_0 - Rt^{\frac{1}{2}} \mathrm{A}_{sub} \qquad 9$$

which can be rearranged to give

$$\exp\left(- bR_b\right) = -\frac{\mathrm{A}_{sub} R}{a} t^{\frac{1}{2}} + \frac{\theta_0}{a} \qquad 10$$

Equation 10 can be used to produce a plot of the function $\exp\left(- bR_b\right)$ *versus* $t^{1/2}$. Figure 1 shows such a plot over 49 min, together with experimentally determined values of R_b also plotted against $t^{1/2}$, from which can be seen that R_b is a curve increasing with

increase in $t^{1/2}$ and that $\exp(-bR_b)$ decreases linearly with increase in $t^{1/2}$. The values typically found in practice are taken as A_{sub} = 6.25x10^{-4} m^2 and R = 4.82 mm.min $^{-1/2}$ [15]. The value of θ_0 used to generate the exponential function was 0.036. The numerical values used for constants a and b were 44.6x10^{-3} and 2.5x10^{-3} respectively.

Sharp Front theory predicts that the water abstracted from the wet mix by the absorbent substrate is linear with $t^{1/2}$. The theory described above predicts that the function $\exp(-bR_b)$ should also be linear with $t^{1/2}$ during dewatering.

3. Experimental Method

3.1 Mortar preparation

Natural hydraulic limes of classification 2, 3.5 and 5 supplied by Hanson Cement Ltd, Clitheroe, UK were used. Mortars were prepared with pre-dried concreting sand consisting of a single source (Croxden) sand having 98.9% of particles < 1.18 mm. The masses of lime and sand needed to produce the required mix proportions by volume were calculated from values of density. To ensure consistency, a standard mixing regime was followed. The lime and sand were mixed by hand for several minutes. The required quantity of water was then added and mixing was continued by hand for a further ten minutes until the constituents were intimately combined. A constant proportion of 1:2 lime:sand by volume was used. Mortar mixes were prepared with water:lime 0.78:1, 0.89:1 and 1:1 by volume.

3.2 Sorptivity

The absorbent substrate material used to dewater the mortars was pressed clay facing brick. The method used to measure the sorptivity S is fully described by Hall and Tse [28]. Individual bricks from the same batch showed considerable variation in sorbtivity.

Samples cut from the same brick exhibited the similar variation. For this reason prisms of square cross section 25 mm were cut parallel to the stretcher face. The prisms were dried to constant weight at 105 ^{o}C. The sorptivity of each prism was measured by placing the end face in contact with a shallow layer of water and removing and weighing at intervals. Sorptivity was determined from the gradient of a graph of the cumulative absorbed volume of water per unit area versus $t^{1/2}$. The sections were then re-dried for mortar placement and impedance measurement. The depth of bed used in the experimental work for each brick prism was sufficient to completely dewater the 45 mm deep mortar.

3.3 Determination of bulk resistance

A test cell consisting of a rectangular plastic container of identical cross sectional area to the brick prism was attached to one end of the prism with adhesive tape. The test cell contained two stainless steel rectangular electrodes each 25 mm in width and 30 mm in height a distance 25 mm apart, as shown in figure 2(a). This gave an electrode area of 625 mm^2. These electrodes were arranged to be 15 mm above the prism face. Mortar was then placed immediately after mixing into the container to a total depth of 45 mm in several stages, tamping after each addition. Figure 2(b) shows a schematic of the test cell arrangement and illustrates the Sharp Front analysis already described.

The impedance of the mortar was monitored using a Solartron 1260 impedance analyser, in stand-alone mode, over the frequency range 10 MHz to 100 Hz at a potential of 100 mV. The time taken for the analyser to complete each sweep was approximately 70 seconds. Sweeps were repeated continuously for 200 minutes. The nulling procedure described in [13] was used to reduce the electrical contributions from the leads and sample holder.

4. Results and Discussion

Typical complex plane impedance data (corrected using the nulling procedure) of NHL5 mortar of composition 1:2:0.78 lime:sand:water at 10, 20, 30 and 60 minutes after placing on the brick prism are given in Figure 3(a). Such plots are interpreted as two arcs the intersection of which on the real impedance axis gives the bulk resistance, R_b, here 170, 233, 270 and 310 Ω respectively. Figure 3(b) shows a plot over an idealised frequency range. The associated equivalent circuit inset shows the model of a resistor and capacitor in parallel associated with each arc. The lower frequency arc on the right hand side is due to the electrode response and the higher frequency arc on left hand side is due to the mortar. For the measurements reported here this intersection occurred at a frequency of 251 kHz and did not change significantly with time. Hence a value for the bulk resistance of the mortar between the electrodes was taken as the real impedance at 251 kHz. Despite the nulling procedure the left hand side semicircles (associated with the mortar) are extremely depressed probably due to some electrical response of the leads.

Figure 4 compares the variation in bulk resistance with the square root of time from placing freshly mixed NHL5 mortar of composition 1:2:0.78 lime:sand:water both on absorbent brick substrate and on non-absorbent polymer sheet over 2.8 hours (13 $min^{1/2}$). No significant change in bulk resistance for the mortar on the polymer sheet is seen over this time. Bulk resistance was constant at 118 +/- 4 Ω. In contrast mortar placed on absorbent brick shows a distinct change in bulk resistance with time. After approximately 30 minutes the rate of increase in bulk resistance decreases. Within this time the absorbent substrate has abstracted some of the mix water and we suggest here that the change in ion concentrations of the remaining solution is reflected in the value of the bulk resistance.

The previously derived function $\exp(-bR_b)$ is plotted against the square root of time from placing freshly mixed mortar on brick prisms. The value 0.1 was taken for constant b in order to give values of the function $\exp(-bR_b)$ between zero and one. Figure 5 is a plot of $\exp(-bR_b)$ versus square root of time since placing NHL2 mortars of water:lime proportions 0.78:1, 0.89:1 and 1:1 and shows the effect of increasing the volume of mix water. Figure 6 shows the same function plotted against the square root of time for the

range of hydrolocity mortars examined, all of mix proportion 0.78:1:2 water:lime:sand. Small variations in sorptivity were found between prisms cut from the same brick and the sorptivity values are given in the figure captions. These variations are likely to have some small influence, which is illustrated by comparing the experimental results for NHL2 mortar (of mix proportion 0.78:1:2) in Figure 5 with that in Figure 7 (lower line) where substrate sorptivity differs by 0.04 $mm.min^{1/2}$. Larger variations in sorptivity do significantly alter dewatering and this effect is shown in Figure 7, which presents a similar plot to those of figures 5 and 6, for NHL2 mortar of 0.78:1:2 water:lime:sand mix proportion on brick prisms of widely different sorptivity.

Each of the figure 5 - 7 shows a smooth curve between two linear regions. For each linear portion the correlation coefficient was at least 0.99. We suggest that the initial linear portion corresponds to dewatering and the second linear portion, the gradient of which is very much smaller, corresponds to the time over which the mortar is no longer losing water to the substrate but during which the concentrations of ion species are changing due to hydration reactions. Hence this gradient is smaller but not zero.

Boltzmann's law has previously been applied to mortars to derive a relationship between water content and measured resistivity [29]. Here the constant *a* is used to represent the influence of water retention on the electrical properties and may be dependent on physical properties which alter this water retention, such as specific surface area, porosity and tortuosity. The constant *b* is related to the chemical properties of pore water solution, such as ionic concentration and the charge on ions in solution. Since the nature and magnitude of the forces influencing water retention vary considerably for different water contents, values of *a* and *b* may well change with volume fraction of water. It is assumed here that *a* and *b* are constant within a certain volume fraction water content but may vary between thin films and bulk solution. In the context of a lime mortar dewatering on a brick substrate the fresh mix is of high volume fraction water content, in this work between 0.2 and 0.25. The dewatered mortar is of lower volume fraction water (and hence higher volume fraction solids) content and may contain a proportion of air. As the

mortar is changing from freshly placed to fully dewatered, changes in a or b may influence the gradient when $\exp(-bR_b)$ is plotted *versus* $t^{½}$ as in Figures 5, 6 and 7.

For the purpose of this study the point at which the extrapolated portions of the two linear sections intersect has been taken as the time at which dewatering is complete *i.e.* when all fresh mix has been converted to filter cake (in the terminology of Figure 2b). It is proposed that the time at which the change in gradient occurs indicates the end of dewatering for the 45 mm depth of mortar. In support of this Table 1 gives the values of desorptivity determined from pressure cell measurements, where these are available, for the identical NHL mortar [15]. Values of the brick sorptivity measured in this study and values of transfer sorptivity between the mortar and the brick prism were calculated using equation 1. Minor variations in sorptivity have a small effect on the transfer sorptivity. Values of time to dewater the 45 mm mortar bed can be calculated from Sharp Front theory using these values of transfer sorptivity and the approach described in [30] and are also given in Table 1 with the time to dewater obtained from the extrapolated linear regions of Figures 5, 6 and 7. The purpose of this table is not to demonstrate exact correspondence between the calculated and measured times to dewater but to present support for the proposal that the impedance method is indeed detecting the end of the dewatering process. Both calculated and measured times to dewater are of similar magnitude and the trend is the same when the hydraulicity of the lime increases, giving confidence that the measurements of bulk resistance do detect the time at which dewatering is complete.

The results presented here showing the effects of proportion of mix water, hydraulicity of lime and sorptivity of substrate on the time to dewater 45 mm bed of mortar correspond with those obtained from transfer sorptivity measurements made by experimental determination of mass and volume on 20 mm depth of mortar [30]. In summary the time to dewater, decreases with increasing hydraulicity of lime, decreases with increased proportion of mix water and decreases when increase in substrate sorptivity is large.

Using the experimental technique described here, and the exponential function derived in the theory section, it is therefore possible to determine the time to dewater a freshly mixed and placed mortar **in situ,** provided there is adequate depth of absorbing substrate.

5. Conclusions

The results demonstrate the use of bulk resistance as a non destructive tool for monitoring changes in freshly mixed hydraulic lime materials placed on absorbent substrates. The results presented show a linear relationship between an exponential function of resistivity and the square root of elapsed time since placing. Predictions based on Sharp Front theory have been experimentally validated. It is suggested that the two linear regions observed in plots of this exponential function correspond to a transition between dewatering of the fresh mix under the influence of the capillary pressure of the substrate and water consumption by hydration reactions. It is also suggested that the time between the two linear regions represents the end of dewatering. The results demonstrate the capability of impedance to determine bulk resistance and to relate this directly to changes in volume fraction water content of mortars, and potentially to the dewatering of slurries in general.

During dewatering of mortars in the freshly mixed state significant changes in both volume fraction water content and particle packing of binder and sand occur within a relatively short time period. We suggest that this dewatering process and subsequent consolidation of the dewatered mortar are crucial to the development of both short and long term properties.

Acknowledgements

The authors acknowledge financial support from EPSRC and Hanson Cement Ltd, Clitheroe, UK, for the supply of materials.

Glossary of terms

S	sorptivity
R	desorptivity
A	transfer sorptivity
i	cumulative volume of water desorbed per unit area of wet mix
t	time
K_c	saturated permeability
Ψi	capillary potential
Lc	depth of filter cake
$A_{sub.}$	area of fresh mix in contact with absorbent substrate
θ_0	initial volume fraction water in the mix
θ	volume fraction of water in the filter cake at time t
N_i and N_j	numbers of constituent ions i and j
E_i and E_j	energies of states i and j.
k	Boltzmann's constant (1.38041×10^{-23} JK^{-1})
T	absolute temperature.
φ	electrical potential
e	the electronic charge
z	summary valence of the mobile ions in solution
ρ	electrical resistivity
a and b	empirical constants
R_b	resistance

9. References

[1] A. El-Turki, R. J. Ball, M. A. Carter, M. A. Wilson, C. Ince and G. C. Allen, Effect of dewatering on the strength of lime and Cement Mortars, *J. Am. Ceram. Soc.* 93 **7** 20-74-2081 (2010)

[2] R. J. Ball, A. El-Turki and G. C. Allen, Influence of carbonation on the load dependent deformation of hydraulic lime mortars. Materials Science and Engineering A, 528 (7-8), 3193-3199 (2011)

[3] C. Hall and W. D. Hoff, *Water Transport in Brick and Concrete*, Spon Press, 29-56, 2002.

[4] C. Ince, M. A. Carter, M. A. Wilson, N. C. Collier, A. El-Turki, R. J. Ball and G. C. Allen, Factors affecting the water retaining characteristics of lime and cement mortars in the freshly-mixed state, Materials and Structures, 44 **2** 509-516 (2011)

[5] R. J. Ball, A. El-Turki, G. C. Allen,. Influence of carbonation on the load dependent deformation of hydraulic lime mortars, Materials Science and Engineering A, 528 **7-8** 3193-3199 (2011)

[6] G. C. Allen, J. Allen, N. Elton, M. Farey, S. Holmes, P. Livesey and M. Radonjic, *Hydraulic Lime Mortar for Stone, Brick and Block Masonry*, Donhead, 2003.

[7] R. J. Ball, A. El-Turki, J. Allen, G. C. Allen, The stress cycling of hydraulic lime mortars, *Const. Mat. Proc. Inst. Civil Eng*., **2**, 67-53 (2007).

[8] A. El-Turki, R. J. Ball, G. C. Allen, The influence of relative humidity on structural and chemical changes during carbonation of hydraulic lime, *Cem. Con. Res*. **37,** 1233-1240 (2007).

[9] W. J. McCarter, S. Garvin and N. Bouzid, Impedance measurements on cement pastes. *J. Mat. Sci. Lett*., **7**, 1056-7 (1988).

[10] W. J. McCarter and R. Brousseau, The AC response of a hardened cement paste. *Cem. Concr. Res*., **20,** [6] 891-900 (1990).

[11] W. J. McCarter, T. M. Chrisp and G. Starrs, The early hydration of alkali activated slag: developments in monitoring techniques, *Cem. Concr. Comp*., **21**, 277-283 (1999).

[12] W. J. McCarter, G. Starrs, G. and T. M. Chrisp, Electrical monitoring methods in cement science. *Structure and Performance of Cements*, J. Benstead and P. Barnes (Eds), SPON, London, 2002.

[13] B. J. Christensen, R. T. Coverdale, R. A. Olson, S. J. Ford, E. J. Garboczi, H. M. Jennings and T. Mason, Impedance Spectroscopy of Hydrating Cement-Based Materials: Measurement, Interpretation, and Application, *J. Am. Ceram. Soc*., **77,** [11] 2789-804 (1994)

[14] R. J. Ball, G. C. Allen, G. Starrs and W. J. McCarter, Forthcoming. Impedance spectroscopy measurements to study physio-chemical processes in lime-based composites. *Applied Physics A Materials Science & Processing* (2011) DOI: 10.1007/s00339-011-6509-7

[15] C. Ince, *Water transport kinetics in mortar-masonry systems*, PhD Thesis, 2009, University of Manchester.

[16] R. P. Ewing, A. G. Hunt, Dependence of the Electrical Conductivity on Saturation in Real Porous Media, *Vados Zone Journal, Soil Science Society of America*, **5**, 731-741 (2006)

[17] F.Ozcep, O. Tezel, M. Asci, Correlation between Electrical Resistivity and Soil-Water Content: Istanbul and Golcuk, *International Journal of Physical Sciences*, 4 (6) 362-365 (2009)

[18] F.Ozcep, E. Yıldırım, O. Tezel, M. Asci, S. Karabulut, , Correlation between Electrical Resistivity and Soil-Water Content based Artificial Intelligent Techniques, *International Journal of Physical Sciences*, Vol. 5 (1), pp. 047 – 056 (2010)

[19] S.I. Siddiqui and V.P. Drnevich, A new method of measuring density and

moisture content of soil using the technique of time domain reflectometry: Final report. West Lafayette, In: Purdue University (1995).

[20] X. Yu, and V.P. Drnevich,. Soil water content and dry density by time domain reflectometry. *Journal of Geotechnical and Geoenvironmental Engineering*, 130 (9) 922-934 (2004)

[21] C. M. K. Gardaner, T. J. Dean and J. D. Cooper, Soil water content measurement with a high-frequency capacitance sensor. *Journal of Agricultural Engineering Research*. 71 (4), 395-403 (1998)

[22] G.J. Cai S.Y. Liu, L.Y. Tong, G.Y. Du. Resistivity cone penetration test technique and data interpretation, *Chinese Journal of Rock Mechanics and Engineering*, 26 (supp1) 3127-3133 (2007)

[23] N. C. Collier, M. A. Wilson, M. A. Carter, W. D. Hoff, C. Hall, R. J. Ball, A. El-Turki and G. C. Allen, Theoretical development and validation of a Sharp Front model of the dewatering of a slurry by an absorbent substrate, *J. Phys. D: Appl. Phys.,* **40**, 4049-4054 (2007).

[24] S. S. Dukhin and B. V. Derjaguin, *Electrokinetic Phenomena*, J. Wiley and Sons, 1974.

[25] R. M. Besanson, (Ed.). *The Encyclopedia of Physics*. Van Norstrand Reinhold Comp. NY, 1974.

[26] M. Tschapek and S. Falasca, Water retention by disperse hydrophilic materials as affected by surface tension, *Powder Technology,* **48**, [3] 1986, 223-226.

[27] D. R. Nielsen, J. W. Jackson, J.W. Cary, and D.D. Evans (Ed.). *Soil water. ASA (American Society of Agronomy), SSSA (Soil Science Society of America),* 677 South

Segoe Road, Madison, Wisconsin, 53711, Chapter 6. Isothermal flow of aqueous solutions, p135, 1972.

[28] C. Hall, T. T. Kam-Ming, Water movement in porous building materials—VII. The sorptivity of mortars, *Build. and Environ*., **21,** [2] 1986, 113-118.

[29] R. J. Ball and G. C. Allen, The measurement of water transport in porous materials using impedance spectroscopy, *J. Phys. D: Appl. Phys*., **43,** (2010), 105503, doi:10.1088/0022-3727/43/10/105503.

[30] C. Ince, M. A. Carter, M. A. Wilson , A. El-Turki, R. J. Ball, G. C. Allen and N. C. Collier Analysis of the abstraction of water from freshly mixed jointing mortars in masonry construction*, Mater. and Struct*. (2009) DOI 10.1617/s11527-009-9560-5.

Table 1. Measured and calculated water transport parameters.

Lime	Mix proportions by volume (water:lime:sand)	Desorptivity ($mm.min^{1/2}$) at 0.05 MPa from [15]	Sorptivity of brick ($mm.min^{1/2}$)	Transfer sorptivity ($mm.min^{1/2}$)	Time to dewater 45 mm (min) [Calculated]	Intercept of linear region ($min^{1/2}$)	Time to dewater 45 mm (min) [Measured]
NHL2	0.78:1:2	1.33	2.27	1.15	55.3	6.66 (Fig 5)	44.3
NHL2	0.89:1:2	-	2.35	-		6.81 (Fig 5)	46.4
NHL2	1:1:2	-	2.38	-		6.96 (Fig 5)	48.5
NHL2	0.78:1:2	1.33	2.27	1.15	55.3	6.66 (Fig 5,6)	44.3
NHL3.5	0.78:1:2	-	2.21	-		6.44 (Fig 6)	42.0
NHL5	0.78:1:2	1.65	2.63	1.40	37.3	5.88 (Fig 6)	35.0
NHL2	0.78:1:2	1.33	1.64	1.03	65.0	7.31 (Fig 7)	53
NHL2	0.78:1:2	1.33	2.31	1.15	55.3	6.78 (Fig 7)	45.9

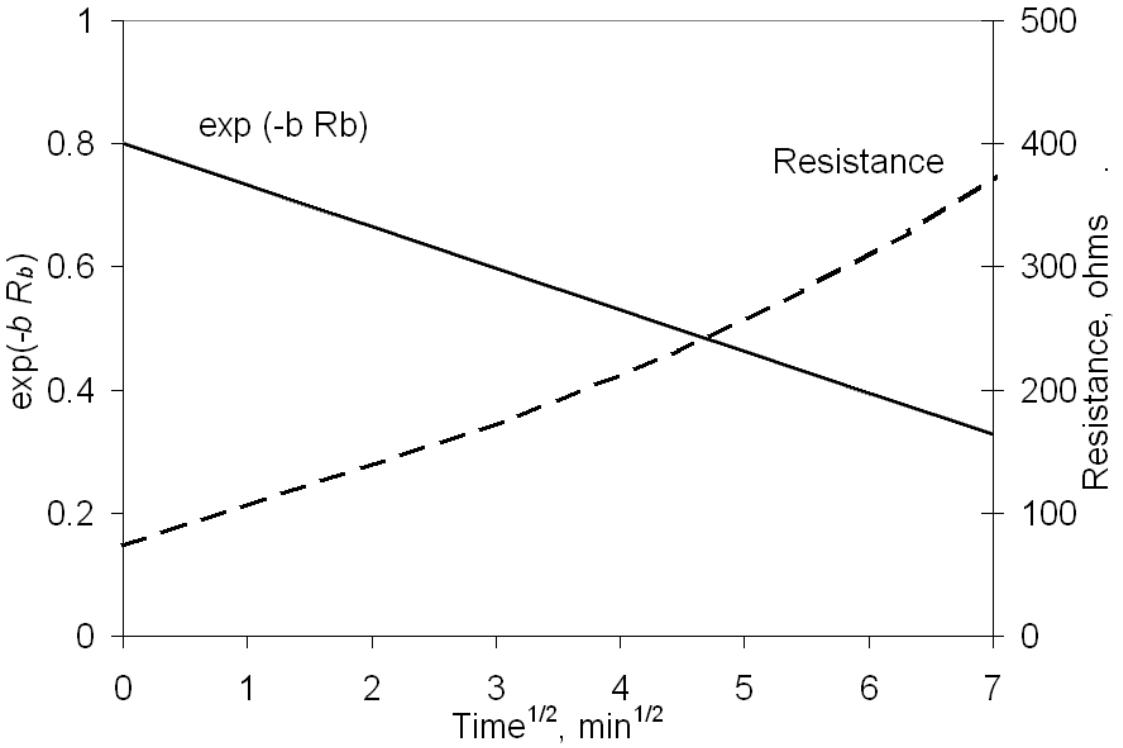

Figure 1. The function exp (-*b* R_b) from equation 10 (solid line) *versus* $t^{1/2}$ time and bulk resistance R_b (dashed line) *versus* $t^{1/2}$.

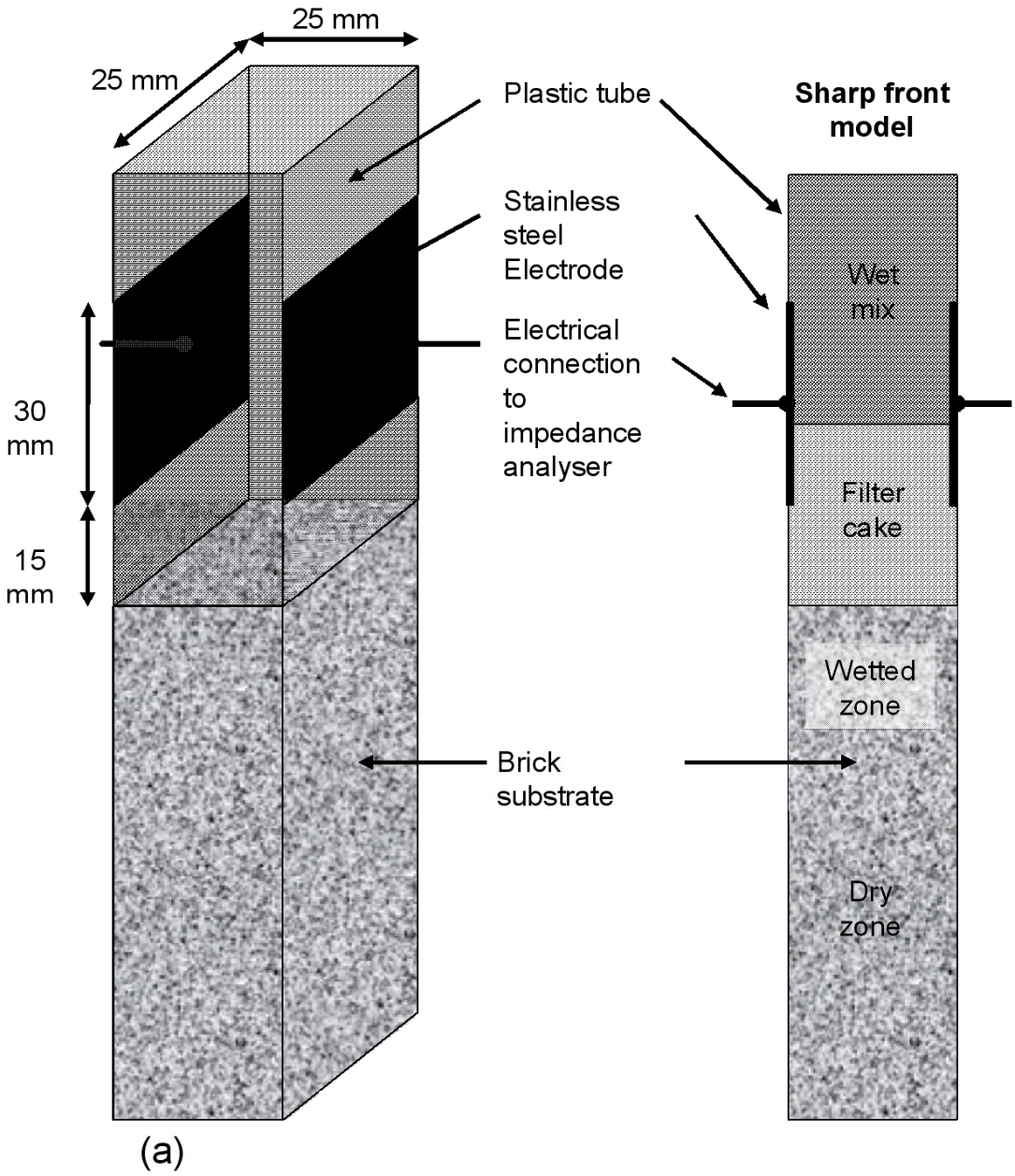

Figure 2. (a) Schematic diagram showing test cell, electrodes and brick prism. (b) Sharp front model of dewatering of mortar. Taken from R. J. Ball and G. C. Allen, *J. Phys. D:* (2010) [17].

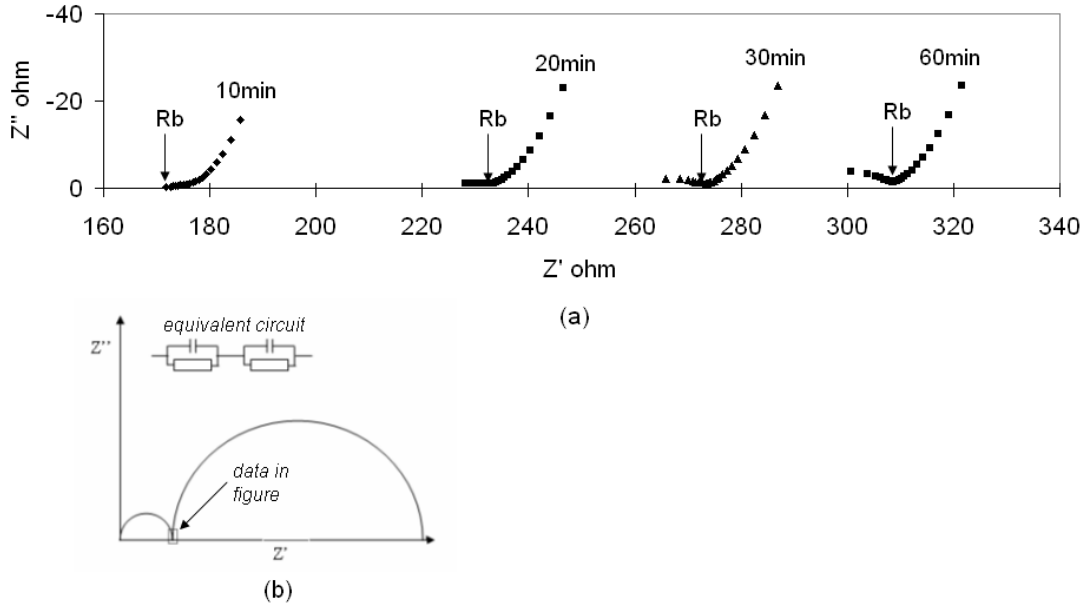

Figure 3. (a) Complex plane plots obtained at 10, 20, 30 and 60 minutes after placing NHL5 mortar on brick prisms. (b) Idealised plot. Frequency range 2.5 MHz to 0.1 kHz. (Real impedance, Z', imaginary impedance Z'')

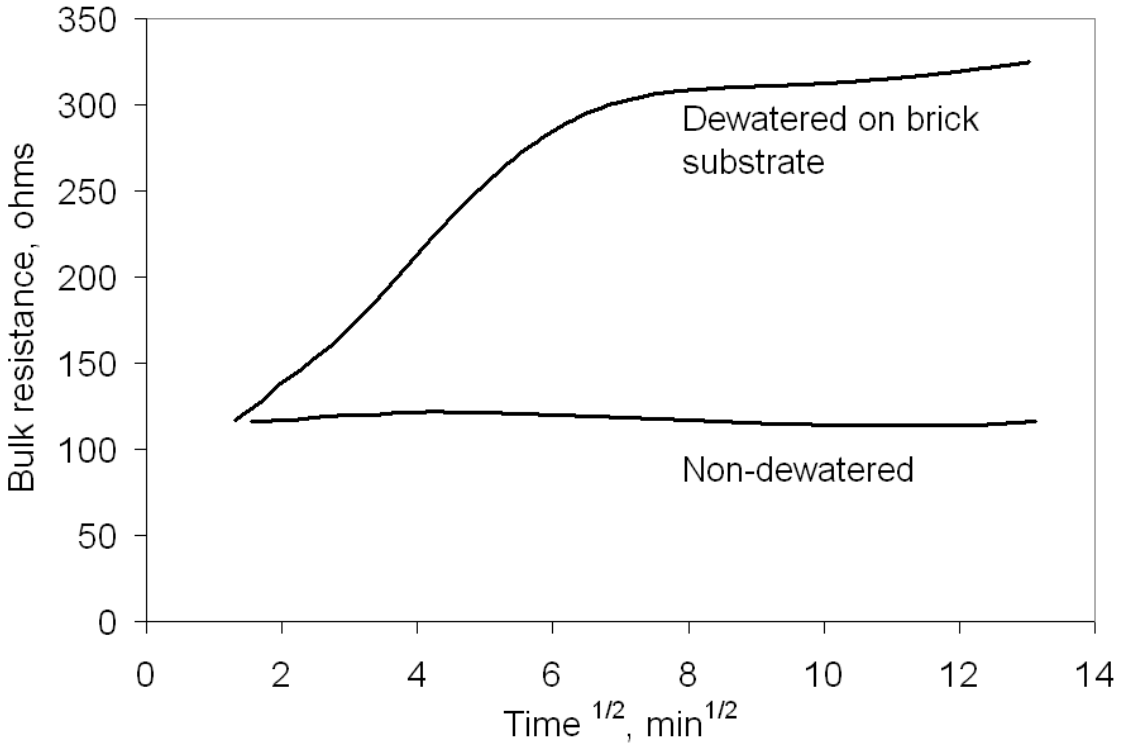

Figure 4. Variation in bulk resistance with $t^{1/2}$ for NHL5 mortar placed on a clay brick substrate (upper line) and a non-absorbent substrate (lower line).

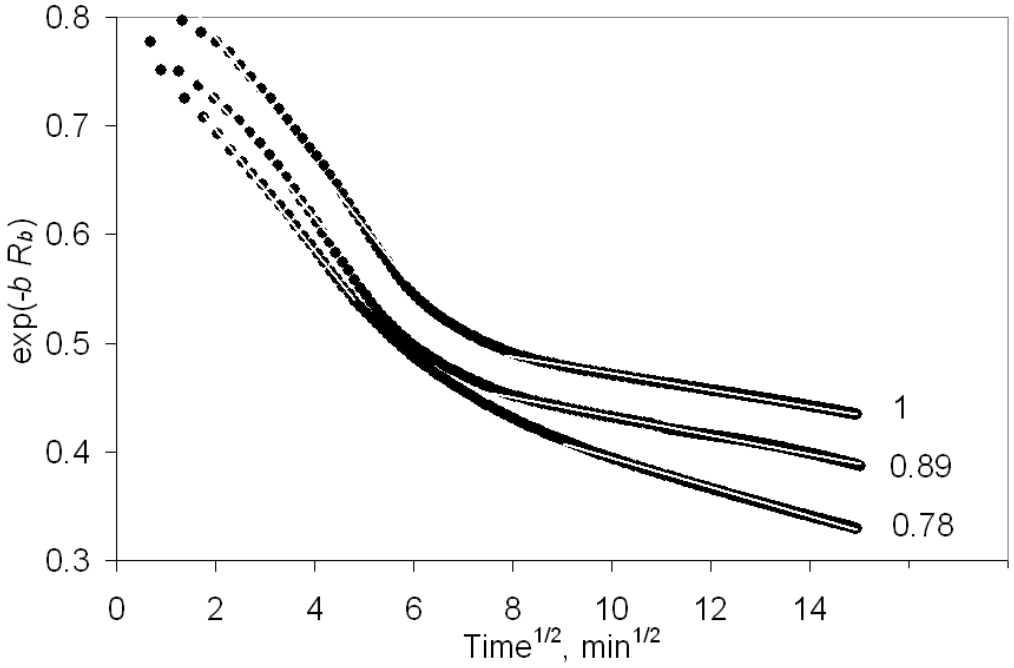

Figure 5. Exp(-b R_b) versus $t^{1/2}$ for NHL2 mortars prepared with water:lime proportions 0.78:1, 0.89:1 and 1:1, dewatered on clay brick prisms of sorptivity of 2.27, 2.35 and 2.38 mm.min$^{0.5}$ respectively. (0.78:1 data are also presented in Figure 6)

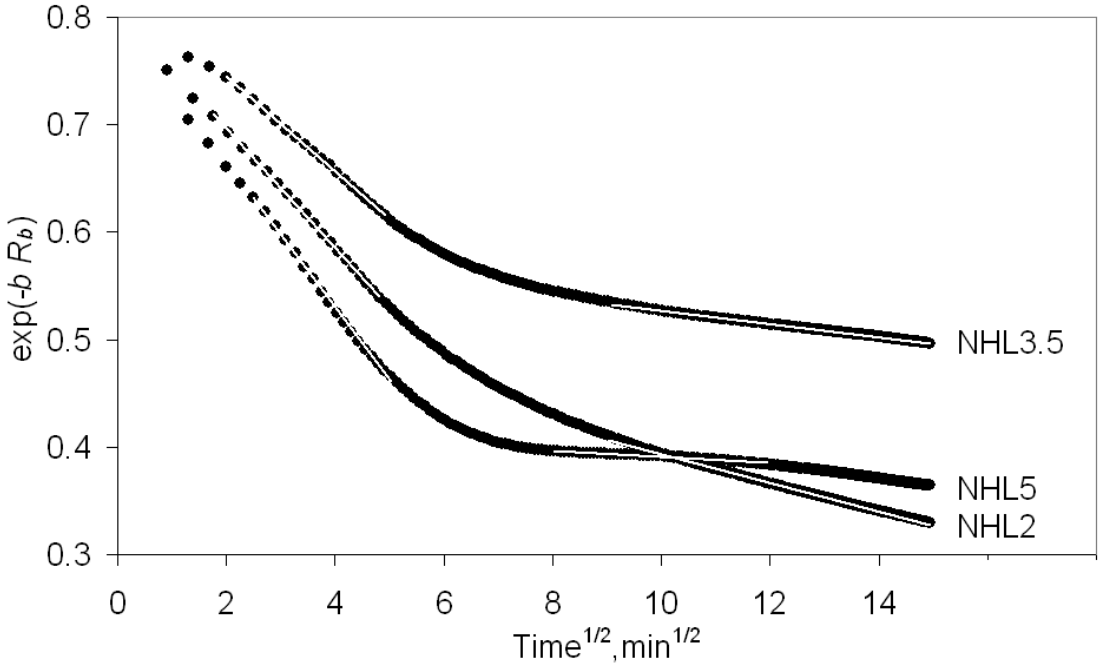

Figure 6. Exp (-*b* R_b) versus $t^{1/2}$ for NHL2, NHL3.5 and NHL5 mortars of composition 1:2:0.78 lime:sand:water dewatered on clay brick prisms. Brick sorptivity 2.27, 2.21, and 2.63 $mm.min^{0.5}$ respectively.

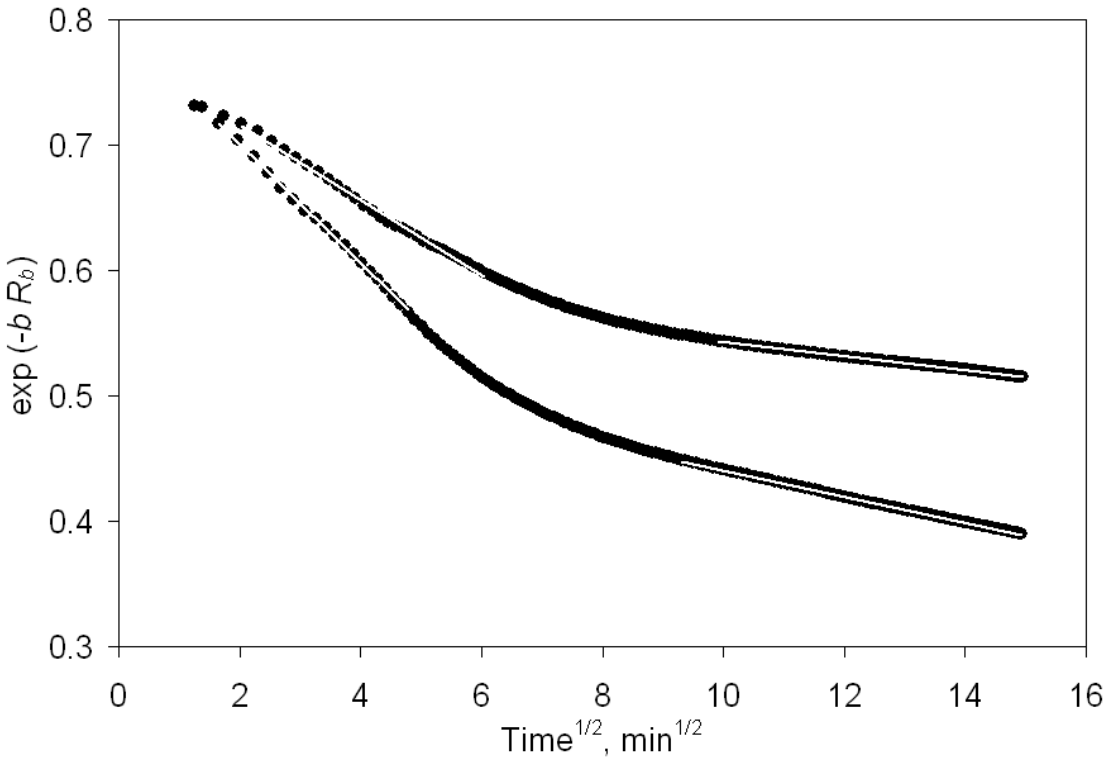

Figure 7. Exp (-*b* R_b) versus $t^{1/2}$ for NHL2 mortar of composition 1:2:0.78 lime:sand:water dewatered on clay brick prisms. Brick sorptivity 1.64 mm.min$^{0.5}$ (upper line), 2.31 mm.min$^{0.5}$ (lower line).